Margatoxin Binds to a Homomultimer of $K_V1.3$ Channels in Jurkat Cells. Comparison with $K_V1.3$ Expressed in CHO Cells†

Lisa M. H. Helms,‡ John P. Felix,‡ Randal M. Bugianesi,‡ Maria L. Garcia,‡ Scott Stevens,‡ Reid J. Leonard,‡ Hans-Günther Knaus,§ Robert Koch,§ Siegmund G. Wanner,§ Gregory J. Kaczorowski,‡ and Robert S. Slaughter*,‡

Department of Membrane Biochemistry and Biophysics, Merck Research Laboratories, P.O. Box 2000, Rahway, New Jersey 07065, and Institute for Biochemical Pharmacology, Peter Mayr-Strasse 1, A6020 Innsbruck, Austria

Received September 17, 1996; Revised Manuscript Received December 19, 1996⊗

ABSTRACT: Voltage-gated potassium (K_V) channels play key roles in setting the resting potential and in the activation cascade of human peripheral T lymphocytes. Margatoxin (MgTX), a 39-amino acid peptide from *Centruroides margaritatus*, is a potent inhibitor of lymphocyte K_V channels. The binding of monoiodotyrosinyl margatoxin ([^{125}I]MgTX) to plasma membranes prepared from either Jurkat cells, a human leukemic T cell line, or CHO cells stably transfected with the *Shaker*-type voltage-gated K^+ channel, $K_V1.3$, has been used to investigate the properties of lymphocyte K_V channels. These data were compared with [^{125}I]MgTX binding to heterotetrameric K_V channels in rat brain synaptic plasma membranes [Knaus, H. G., et al. (1995) *Biochemistry 34*, 13627−13634]. The affinity for [^{125}I]MgTX is 100−200 fM in either Jurkat or CHO/$K_V1.3$ membranes, and the receptor density is 20−120 fmol/mg in Jurkat membranes or 1000 fmol/mg in CHO/$K_V1.3$ membranes. In contrast to rat brain, [^{125}I]MgTX binding to Jurkat and CHO/$K_V1.3$ membranes exhibits an absolute requirement for K^+, with no potentiation of binding by Na^+. $K_V1.3$ was the only K_V1 series channel present in either CHO/$K_V1.3$ or Jurkat plasma membranes as determined by immunoprecipitation of [^{125}I]MgTX binding or by Western blot analyses using sequence-specific antibodies prepared against members of the K_V1 family. The relative potencies of a series of peptidyl K_V channel inhibitors was essentially the same for inhibition of [^{125}I]MgTX binding to Jurkat, CHO, or rat brain membranes and for blocking $^{86}Rb^+$ efflux from the CHO/$K_V1.3$ cells, except that α-dendrotoxin was more potent at blocking binding to rat brain membranes than in the other assays. The characteristics of [^{125}I]MgTX binding, the antibody profiles, and the effects of the peptidyl K_V inhibitors all indicate that the [^{125}I]MgTX receptor in Jurkat lymphocytes is comprised of a homomultimer of $K_V1.3$, unlike the heteromultimeric arrangement of the receptor in rat brain.

Margatoxin (MgTX),[1] a 39-amino acid peptide purified from the venom of the scorpion, *Centruroides margaritatus*, is a selective potassium channel inhibitor (Garcia-Calvo et al., 1993). Of the channels tested, MgTX potently blocks only $K_V1.2$ (M. L. Garcia, R. J. Leonard, and O. McManus, unpublished observations) and $K_V1.3$, members of the *Shaker* family of voltage-gated potassium (K_V) channels. $K_V1.3$ has been identified in human (Attali et al., 1992), mouse (Chandy et al., 1990), and rat (Swanson et al., 1990) T cells and is thought to be responsible for the n-type current recorded in lymphocytes (Grissmer et al., 1990). MgTX has been reported to depolarize human peripheral blood T lymphocytes (Leonard et al., 1992), indicating that $K_V1.3$ sets the resting potential of these cells. When T cells are stimulated at the level of the T cell receptor, depolarization elicited either by inhibition of lymphocyte K_V channels or by raising extracellular K^+ blocks the rise in $Ca^{2+}{}_i$ required for activation (Lin et al., 1993). MgTX does not exhibit the equivocal effects of another K^+ channel inhibitory peptide, charybdotoxin (ChTX), which also blocks T cell activation (Price et al., 1989); unlike ChTX, MgTX does not inhibit calcium-activated K^+ channels which are also found in T cells (Leonard et al., 1992). Not only does MgTX block T cell activation, but also a recent report (Koo et al., 1996) indicates that MgTX inhibits an *in vivo* delayed-type hypersensitivity reaction in Yucatan minipigs. Lymphocyte K_V channels, then, are a pivotal site for the control of T cell activation, and MgTX is a specific inhibitor of this process.

The receptor for the monoiodinated form of MgTX ([^{125}I]-MgTX) has recently been characterized in rat brain synaptic plasma membranes (Knaus et al., 1995). [^{125}I]MgTX binds to synaptic membranes with very high affinity, and bound [^{125}I]MgTX can be immunoprecipitated by antibodies to either $K_V1.3$ or $K_V1.2$. These data, along with the pharmacological properties of the binding reaction, indicate that [^{125}I]-MgTX binding in brain is to heteromultimeric channels, some of which are comprised of $K_V1.3$ and $K_V1.2$ subunits. Thus, questions are raised as to the properties of the [^{125}I]MgTX binding site as well as to its subunit composition in T lymphocytes.

† Supported by an APART fellowship from the Austrian Academy of Sciences and Grants S6611-MED and P11197-MED from the Austrian Research Foundation.

* Author to whom correspondence should be addressed.

‡ Merck Research Laboratries.

§ Institute for Biochemical Pharmacology.

⊗ Abstract published in *Advance ACS Abstracts,* March 15, 1997.

[1] Abbreviations: NBT, nitro blue tetrazolium; BCIP, 5-bromo-4-chloro-3-indolyl phosphate; Tris, tris(hydroxymethyl)aminomethane; HEPES, 4-(2-hydroxyethyl)-1-piperazineethanesulfonic acid; SDS/PAGE, sodium dodecyl sulfate/polyacrylamide gel electrophoresis; K_V, voltage-gated potassium channel; K_V1 series, *Shaker* series of voltage-gated potassium channels; MgTX, margatoxin; [^{125}I]MgTX, monoiodinated margatoxin; [^{125}I]$_2$MgTX, di-iodinated margatoxin; ChTX, charybdotoxin; AgTX-1, agitoxin-1; AgTX-2, agitoxin-2; NxTX, noxiustoxin; KTX, kaliotoxin; α-DaTX, α-dendrotoxin; IbTX, iberiotoxin; HPLC, high-performance liquid chromatography; TFA, trifluoroacetic acid; BSA, bovine serum albumin; DTT, dithiothreitol; EDTA, ethylenedinitrilotetraacetic acid; EGTA, ethylene glycol bis-(β-aminoethyl ether)-*N*,*N*,*N*′,*N*′-tetraacetic acid.

S0006-2960(96)02351-3 CCC: $14.00

In this study, [^{125}I]MgTX binding was characterized and compared in plasma membranes prepared from either Jurkat, a human T cell leukemia line, or CHO cells stably transfected with K_V1.3. Binding properties of [^{125}I]MgTX are identical in these two membrane preparations with respect to affinity, salt dependence, and the ability of a series of peptidyl K_V channel inhibitors to inhibit [^{125}I]MgTX binding. This latter property is reflected in the ability of the same toxins to block $^{86}Rb^+$ efflux from CHO/K_V1.3 cells. [^{125}I]MgTX binding to Jurkat membrane preparations is immunoprecipitated only by K_V1.3 antibodies. These data for Jurkat or CHO/K_V1.3 membranes contrast with data from rat brain synaptic plasma membranes (Knaus et al., 1995) in that [^{125}I]MgTX binding requires the presence of KCl, is not stimulated by NaCl, and is only weakly inhibited by α-dendrotoxin (α-DaTX). Taken together, the binding and immunoprecipitation data indicate that the lymphocyte [^{125}I]MgTX receptor is a homomultimer of K_V1.3 subunits, in contrast to the heteromultimeric arrangement of K_V channels found in rat brain. A preliminary report of these findings has been made in abstract form (Felix et al., 1995).

MATERIALS AND METHODS

Materials. Compounds used in binding assays were purchased from commercial sources and were of reagent grade or better. HPLC solvents were of HPLC grade. Synthetic MgTX was obtained as previously described (Bednarek et al., 1994).

Preparation of [^{125}I]MgTX. Iodination reagents were made up in iodination buffer which was 200 mM $NaH_2PO_4 \cdot H_2O$ at pH 8.0 with NaOH. The iodination was initiated by the addition of 1 μL (100 mg/mL) β-D-glucose to a mixture containing 2 μL of Enzymobeads (Bio-Rad, control number 72901A, 18 μL iodination buffer/vial), 2 μL of 2 mM MgTX, and 2 mCi (~6 μL, 0.92 nmol) of Na^{125}I (Du Pont/NEN, NEZ-033L). After 20 min at room temperature, 100 μL of iodination buffer was added and the Enzymobeads were removed by centrifugation for 30 s. The supernatant and an additional 100 μL wash were subjected to reversed phase chromatography on a C18 column (Vydak, 5 μm, 0.46 × 25 cm). After sample injection, the column was washed for 30 min with 98% solution A (0.0769% TFA in H_2O) and 2% solution B (0.064% TFA in 35% acetonitrile in H_2O) at a flow rate of 1.5 mL/min. Separation was achieved by an isocratic mixture of 60% A and 40% B for the unlabeled MgTX 55% A and 45% B (Figure 1; mixture switched when the unlabeled peak was 80% eluted) for the monoiodinated and 50% A and 50% B for the di-iodinated form of the peptide. Samples were collected into tubes containing 300 μL of 11X resuspension solution (1100 mM NaCl, 220 mM HEPES, and 1.1% BSA, adjusted to pH 8.0 with NaOH). Samples were lyophilized, resuspended in H_2O, and stored at −70 °C.

Characterization of [^{127}I]MgTX. Reaction conditions with ^{127}INa are as indicated above for ^{125}INa. The two major peaks that eluted after native MgTX were reduced with DTT and carboxymethylated as described (Garcia-Calvo et al., 1993). Reduced carboxymethylated peptides were purified by HPLC and digested with endoproteinase Lys C. Proteolytic fragments were separated by HPLC and subjected to Edman degradation to determine their amino acid sequence.

Preparation of Plasma Membranes from Jurkat Cells. Parts of this procedure are based on a method used for Jurkat cell homogenates (Slaughter et al., 1991). Membrane preparations were performed at 0−5 °C. Jurkat cells were grown in suspension in ISCOV's media with 5% FBS, harvested with a tangential flow membrane, and washed twice in PBS (2000g_{max} for 15 min). Cells were incubated in hypotonic lysing buffer (1 mM $MgCl_2$, 1 mM $CaCl_2$, and 10 mM HEPES at pH 7.5 with HCl) for 10 min and homogenized with a Dounce glass/glass homogenizer, followed by centrifugation at 2000g_{max} for 15 min. After resuspension in lysing buffer, the pellet was subjected to another cycle of homogenization and centrifugation. Combined supernatants were centrifuged at 15000g_{max} for 15 min, and the supernatant was pelleted at 190000g_{max} for 90 min. The pellet was resuspended in gradient buffer (10 mM EDTA, 10 mM EGTA, and 40 mM HEPES at pH 7.4 with HCl) containing 8% sucrose and then homogenized with a Potter-Elvehjem Teflon/glass homogenizer. This homogenate was passed over a discrete sucrose gradient of 35 and 50% at 131000g_{max} for 90 min. Membranes were collected at the 8−35% (Jurkat fraction 1) and 35−50% (Jurkat fraction 2) interfaces and washed in 160 mM NaCl and 20 mM HEPES/Tris at pH 7.4, with centrifugation at 190000g_{max} for 90 min. The pellets were resuspended in the same NaCl solution and rehomogenized with a teflon/glass homogenizer. Aliquots were frozen in liquid nitrogen and stored at −70 °C. Jurkat fraction 1 was used for the experiments reported in this study.

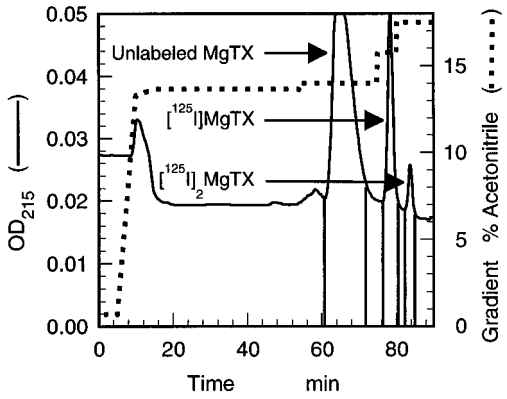

FIGURE 1: Elution profile of [^{125}I]MgTX. MgTX was labeled with ^{125}I and passed through a Vydac C18 reversed phase HPLC column as described in Materials and Methods. The first major peak is the unlabeled MgTX, followed by the monoiodinated form and then the di-iodinated form.

Transfection of K_V1.3 into CHO Cells. CHO/K_V1.3 cells were prepared by the method of DeFarias et al. (1995). These cells were further subcloned to produce a line, 6D94, with approximately 100 000 [^{125}I]MgTX binding sites/cell. This line, 6D94, was used for most of the experiments described in this paper.

Preparation of Plasma Membranes from CHO/K_V1.3 Cells. Initial crude membrane preparation steps are based on a previously reported procedure (Sun et al., 1994). CHO/K_V1.3 cells were grown as previously described (DeFarias et al., 1995), except that 850 cm^2 roller bottles were used. Following a rinse, ~5 mL of PBS was added and cells were scraped from the bottles. Cells were collected by centrifugation at 370g_{max} for 20 min and then resuspended into hypotonic lysis buffer (2 mL/bottle used; 1 mM $MgCl_2 \cdot 6H_2O$, 1 mM EGTA, and 10 mM Tris at pH 7.4 with HCl) with aprotinin (5 μg/mL final concentration) and leupeptin (4 μg/mL final concentration). For the initial step in breaking the cells, the cell suspension was rapidly frozen in liquid

nitrogen and allowed to thaw slowly after a 5-fold dilution into lysing buffer. These suspensions were homogenized with a Polytron PT-35 instrument, setting of 6, for three 10 s bursts interspersed with 10 s intervals, and then subjected to centrifugation at $370g_{max}$, after which the pellet underwent another cycle on the Polytron instrument. The combined supernatants were passed through a centrifugation of $10000g_{max}$ for 20 min and then pelleted by centrifugation at $186000g_{max}$ for 90 min. The pellets were resuspended in lysing buffer with 8% sucrose, homogenized in a teflon/glass homogenizer, layered over a step gradient of 20 and 40% sucrose, and subjected to centrifugation at $130000g_{max}$ for 90 min. The 8−20% (CHO fraction 1) and 20−40% (CHO fraction 2) interfaces were collected, diluted at least 3-fold in storage buffer (160 mM NaCl and 20 mM HEPES at pH 7.4 with NaOH), and pelleted at $186000g_{max}$ for 90 min. Pellets were resuspended in storage buffer, rehomogenized, aliquoted, frozen in liquid nitrogen, and stored at −70 °C. CHO fraction 2 contained the receptor used for this study.

Binding Assays for [^{125}I]MgTX. Unless otherwise stated, membranes were incubated in a total volume of 12 mL with [^{125}I]MgTX in low-salt binding buffer (5 mM KCl, 20 mM Tris-HCl, and 0.2% BSA at pH 7.4) for 2 h at room temperature. The high 12 mL binding reaction volume was required to provide a usable signal under conditions in which only a low percentage of the added ligand was bound even at the lowest ligand concentrations tested. Nonspecific binding was determined in the presence of 10 nM MgTX. Competing peptides were diluted from stock solutions in 100 mM NaCl and 20 mM Tris-HCl at pH 7.4 with 0.1% BSA. Binding reactions were terminated by passing the binding solution through Whatman 25 mm GF/C filters that had been presoaked with 0.5% polyethylenimine and collecting the membranes or cells on the filters. The tubes were then rinsed by the addition of 4 mL of ice-cold quench solution (100 mM NaCl and 20 mM Tris-HCl at pH 7.4), and each rinse was also passed through the filters. The filters were then rinsed three times with 4 mL of ice-cold quench solution. [^{125}I]MgTX bound to the filters was determined by γ counting.

Efflux of $^{86}Rb^+$ from CHO/$K_V1.3$ cells. CHO/$K_V1.3$ cells were plated into 96-well culture plates and maintained in ISCOVE's Modified Dulbecco's Medium (IMDM, with L-glutamine and HEPES, JRH Biosciences). Cells were incubated overnight with $^{86}Rb^+$ (3 μCi/mL, Du Pont-NEN). After aspiration of the media, 100 μL of low-K^+ buffer (containing, in millimolar, 6.5 KCl, 125 NaCl, 1 $CaCl_2$, 2 $MgCl_2$, and 10 HEPES, with the pH adjusted to 7.2 with NaOH), including test samples, 0.2% BSA, and 2 mM ouabain was added. After a 10 min preincubation, $K_V1.3$ channels were opened by depolarization of the cells with high-K^+ buffer (final concentrations of, in millimolar, 63.25 KCl, 68.25 NaCl, 1 $CaCl_2$, 2 $MgCl_2$, and 10 HEPES, with the pH adjusted to 7.2 with NaOH) also containing test peptides. To measure $^{86}Rb^+$ efflux, 100 μL aliquots from each well were added to plates containing 100 μL of MicroScint-40 (Packard) for counting by liquid scintillation techniques. The remaining $^{86}Rb^+$ content of the cells was determined by the addition of 100 μL of MicroScint-40 to each well. Efflux counts were normalized with respect to total counts in the efflux solution plus those in the cells. Activity was determined by the percent inhibition of efflux that is inhibitable by MgTX.

Immunoblot Analysis. Proteins were transferred under constant cooling in 25 mM Tris, 192 mM glycine, and 10% (v/v) methanol from polyacrylamide gels onto PVDF membranes (Immobilon, BioRad, Richmond, CA) for 60 min at a 100 V constant voltage using a mini trans-blot cell (BioRad). After protein transfer, the PVDF membrane was incubated with 10% skim milk powder, 0.5% (w/v) Triton X-100, and 0.1% (w/v) Tween 20 dissolved in 20 mM Tris-HCl (pH 7.4) and 150 mM NaCl (TBS) for 12−18 h at 4 °C. Subsequently, the immunoblot was incubated with a sequence-directed anti-$K_V1.3$ antibody [peptide sequence QHL SSS AEE LRK ARS NST L [anti-$K_V1.3_{(456-474)}$]; amino acid numbering according to Stuhmer et al. (1989)], diluted in the same buffer for 8−12 h at 22 °C. The blots were washed three times with 0.5% Triton X-100 and 0.1% Tween 20 in TBS and incubated with affinity-purified alkaline phosphatase-conjugated goat anti-rabbit IgG at a 1:2000 dilution for 120 min at 22 °C. After washing six times with the buffer described above, the blots were developed in 100 mM Tris-HCl (pH 9.5), 100 mM NaCl, 5 mM $MgCl_2$, 0.033% NBT, and 0.017% BCIP, until the bands of interest were clearly visible (∼10 min). The reaction was stopped by addition of 0.5 M EDTA/Tris at pH 7.4 to final concentration of 20 mM.

Protein Determination. Protein was determined by the amido blue-black method of Schaffner and Weissmann (1973), as modified by Newman et al. (1982).

Data Analysis. Data analyses were performed using DeltaGraph Pro 3.5. Specific binding in saturation binding plots is analyzed with $B = B_{max}/[1 + (K_d/L)^{n_H}]$ (Cheng & Prusoff, 1973), where B_{max} is the maximum binding, K_d the dissociation constant, n_H the pseudo-Hill coefficient, and L the free ligand concentration. Nonspecific binding is determined by linear regression, and total binding is determined with $B = B_{max}/[1 + (K_d/L)^{n_H}] + (\text{nonspecific slope})L$, where the slope is from the nonspecific binding fit. Scatchard analysis was fitted by linear regression. IC_{50}'s for peptide toxins were determined with the equation $B = (B_{eq} - B_{min})/[1 + (I/IC_{50})^{n_H}] + B_{min}$, where B_{eq} is the binding at the ligand concentration tested with no inhibitors present, B_{min} the minimum amount of ligand bound at higher concentrations of inhibitor where the binding curve has leveled off, I the inhibitor concentration, and IC_{50} the inhibition constant. For the data presented, B_{max} was usually around 100% and B_{min} was 0%. The dissociation rate constant, k_{-1}, was determined from the slope of the plot from the first-order decay equation $\ln(B/B_0) = -k_{-1}t$, where B is the amount bound at time t, and B_0 is the value at $t = 0$. The association rate constant, k_1, was determined from plot of $\ln[B_e/(B_e - B)] = (k'_1 + k_{-1})t = k_{obs}t$ and $k_1 = k'_1/L_T$, where B_e is the amount bound at equilibrium, k'_1 is a calculation parameter defined in the original equation, k_{obs} is the observed slope from the linear transformation, and L_T is the total ligand concentration used for the association rate experiment.

RESULTS

Iodination of MgTX. Although ChTX has been used to study lymphocyte K_V channels (Deutsch et al., 1991), MgTX is a more appropriate ligand for this purpose. Unlike ChTX, MgTX is known to only inhibit $K_V1.3$ and not the Ca^{2+}-activated K^+ channels present in lymphocytes (Leonard et al., 1992). In addition, MgTX is significantly more potent as a blocker of $K_V1.3$ than ChTX. In general, MgTX is a

more specific K_V channel ligand than is ChTX. Therefore, MgTX was radiolabeled with ^{125}I to investigate properties of the presumed $K_V1.3$ binding site in T cells.

For optimal iodination of MgTX, high concentrations of reagents are necessary (Materials and Methods). These conditions produce maximum yields without various oxidative byproducts that are seen in more dilute reaction mixtures. Isocratic elution is necessary to obtain adequate separation of the iodinated fractions by HPLC on a C18 column as shown in Figure 1. All attempts at elution of peptides by even a shallow gradient result in incomplete separation of the iodinated and unlabeled MgTX fractions. Only two fractions containing ^{125}I are recovered from the C18 column, and no additional peaks are observed after further elution by additional isocratic steps.

In the MgTX sequence, there are only two possible iodination sites, tyrosine$_{37}$ and the C-terminal histidine$_{39}$. We subjected samples of the two iodinated peaks and native MgTX to mass spectroscopy. For native MgTX, the observed mass was 4185.8 Da, and for the major and second iodinated peaks, the corresponding masses were 4311.5 and 4435.4 Da, respectively. These data indicate that the major iodinated peak contains a single iodine whereas the second peak represents the di-iodo derivative of MgTX. The composition of the major iodinated peak (Figure 1) was defined by sequencing the HPLC-purified C-terminal tetrapeptide after proteolytic digestion as described in Materials and Methods. Edman degradation indicated that the retention time of the residue corresponding to the position of Tyr in the native toxin had been altered, suggesting that it was covalently modified by incorporation of iodine. These experiments indicate that the Tyr residue was the only modified amino acid in the peptide in the first peak eluting after unlabeled MgTX and that it contained a single iodine. Identical experiments were carried out to determine the composition of the second iodinated peak. This peak was determined to be the di-iodinated tyrosine adduct.

Iodination is usually optimized for the monoiodotyrosine [^{125}I]MgTX by using a concentration of MgTX greater than the concentration of ^{125}I. Lower levels of MgTX result in the formation of more of the di-iodinated peak ([^{125}I]$_2$MgTX), both proportionally and in absolute recovery. With this method, the amount of ^{125}I incorporated into MgTX varies from 50 to 80%, in part depending on the batch of Enzymobeads.

Jurkat Binding Characteristics. Jurkat cells are a human T cell leukemia line which has been used to study the lymphocyte K_V channel (Lewis & Cahalan, 1990). Plasma membranes prepared from these cells exhibit high-affinity saturable binding when they are incubated with [^{125}I]MgTX in a medium containing low salt (5 mM KCl and 20 mM Tris-HCl at pH 7.2; Figure 2, upper panels). There is a high ratio of specific binding as compared to nonspecific interactions within the parameter determination range. Values for binding affinity and site density were the same whether determined from the three-parameter curve fit based on the saturation equation or linear regression of the Scatchard analysis (Materials and Methods). In low-KCl Tris binding buffer, the K_d for [^{125}I]MgTX binding to Jurkat membranes is 95 fM with a B_{max} of 35 fmol/(mg of protein) for the experiment shown. B_{max} varies from 20 to 120 fmol/(mg of protein) among different Jurkat membrane preparations (B_{max} and K_d for the currently used preparation are 27.3 ± 5.6 fmol/(mg of protein) and 71 ± 24 fM, respectively), which may

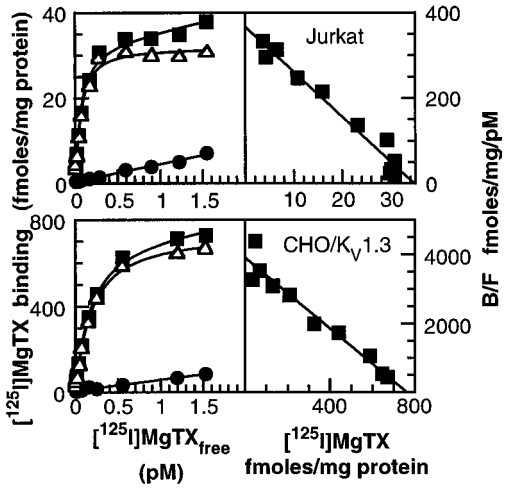

FIGURE 2: Equilibrium binding of [^{125}I]MgTX in low-salt buffer to plasma membranes prepared from Jurkat (upper panels) and CHO/$K_V1.3$ (lower panels). In the saturation plots (left panels), the filled circles represent nonspecific binding in the presence of 10 nM unlabeled MgTX, the filled squares represent the total binding, and the open triangles represent the specific binding. Scatchard analyses of the same data are shown in the right panels.

reflect variability in the expression of the binding site in Jurkat cells (cell binding data supporting this conclusion are not shown). The affinity of [^{125}I]MgTX in Jurkat membranes is similar to that previously found for binding of this ligand to rat brain synaptic membranes under similar experimental conditions. However, the site density in Jurkat membranes is significantly lower than that found in rat brain membranes which were reported as 700−1100 fmol/(mg of protein) (Knaus et al., 1995).

A significant difference between the properties of [^{125}I]-MgTX binding to Jurkat and brain membranes has been observed in the ionic dependence of the binding reaction. At a near physiological salt concentration with 100 mM NaCl and 4.6 mM KCl, using the same membrane preparation as was used in Figure 2, K_d rises from 95 fM to 86 pM (average of 43.6 ± 28.5 pM) for the Jurkat plasma membranes, while the B_{max} at 32 fmol/mg is not significantly changed (Figure 3, upper panels). Increasing either the concentration of NaCl in the presence of a stimulating concentration of KCl or the concentration of KCl by itself above the maximally stimulating concentration reduces [^{125}I]MgTX binding as shown in Figure 4 (upper panel). These effects of NaCl and KCl on [^{125}I]MgTX binding to Jurkat plasma membranes parallel the effects of these monovalent cations in inhibiting the binding to rat brain plasma membranes (Knaus et al., 1995). However, cation effects on [^{125}I]MgTX binding to Jurkat membranes differ in two respects from binding in brain. Since there is no observable [^{125}I]MgTX binding to Jurkat membranes at low KCl concentrations, there is an absolute requirement for the presence of KCl in the binding reaction; there is no stimulation of binding by NaCl at low or any other concentration tested as is found in brain (Figure 4, upper panel).

Binding of [^{125}I]MgTX to Jurkat plasma membranes requires K^+. There is no [^{125}I]MgTX binding at K^+ concentrations below 0.03 mM. The half-stimulation value is 2.1 mM; the optimum is between 3 and 10 mM, and the maximal binding is inhibited at higher concentrations with an IC_{50} of 44 mM (Figure 4, upper panel). The cation requirement in Jurkat membranes is specific for K^+ because Na^+ does not exhibit stimulation of [^{125}I]MgTX binding. In

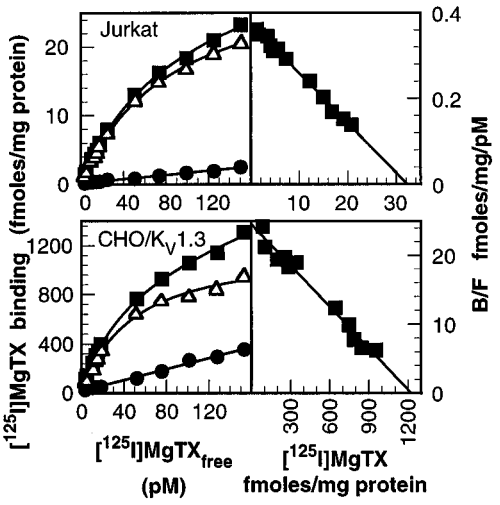

FIGURE 3: Equilibrium binding of [^{125}I]MgTX in high-salt buffer to plasma membranes prepared from Jurkat (upper panels) and CHO/K_V1.3 (lower panels). In the saturation plots (left panels), the filled circles represent nonspecific binding in the presence of 10 nM unlabeled MgTX, the filled squares represent the total binding, and the open triangles represent the specific binding. Scatchard analyses of the same data are shown in the right panels.

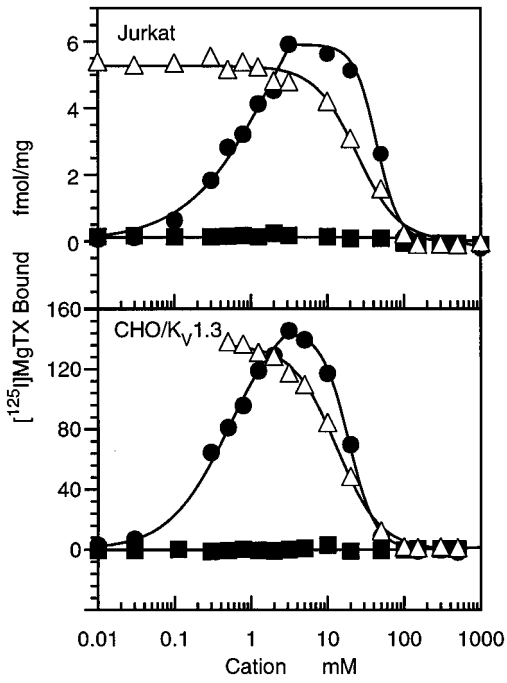

FIGURE 4: Salt dependence of [^{125}I]MgTX binding to plasma membranes prepared from Jurkat (upper panel) and CHO/K_V1.3 (lower panel). Binding is shown in the presence of increasing concentrations of Na^+ (filled squares), K^+ (filled circles), and Na^+ in the presence of a fixed (3 mM) concentration of K^+ (open triangles).

rat brain synaptic membranes, on the other hand, [^{125}I]MgTX binding is enhanced by Na^+ as well as by K^+, and there is significant binding even when neither cation is present (Knaus et al., 1995). In the presence of a stimulatory concentration of K^+ at 3 mM, Na^+ above 10 mM causes a decrease in binding in Jurkat membranes. The toxin affinity is decreased about 1000-fold in 100 mM NaCl and 4.6 mM KCl, where the [^{125}I]MgTX K_d is 86 pM, with no significant differences in B_{max} (Figure 3, upper panel). [^{125}I]MgTX binding is also inhibited in the presence of higher concentrations of KCl. These effects of high salt are similar to those found in rat brain synaptic membranes. Since the rat brain [^{125}I]MgTX receptor has been characterized as a heteromultimeric structure of at least $K_V1.3$ and $K_V1.2$ subunits, the absolute requirement for K^+ to enable binding to Jurkat membranes may reflect the different nature of the receptor complex in the two tissues.

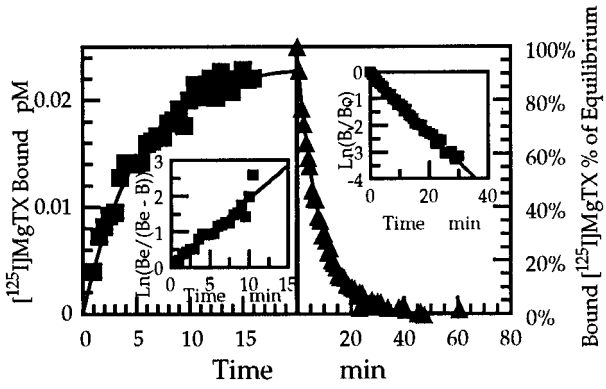

FIGURE 5: Association and dissociation of [^{125}I]MgTX from CHO/K_V1.3 plasma membranes. The association of 140 fM [^{125}I]MgTX under low-salt binding conditions is shown in the left panel. The pseudo-first-order linear transformation is shown in the inset. Dissociation of bound 0.3 pM [^{125}I]MgTX in the presence of 300 pM unlabeled MgTX is shown in the right panel. The inset shows the first-order decay linear transformation.

Characterization of $K_V1.3$ Channels Stably Transfected into CHO Cell Lines. A cell line expressing high levels of $K_V1.3$ was constructed to facilitate the investigation of this channel using flux techniques since both native human peripheral blood T cells and Jurkat cells have a channel density too low to generate a useful signal to noise ratio in such experiments. This cell line would allow the determination of the properties of a $K_V1.3$ homomultimer without the complication of having other K_V1 series channels present that could form heteromultimeric structures. In addition, membranes could be prepared with a much higher site density than would be available from Jurkat membranes.

After transfection, those clones which displayed the highest level of [^{125}I]MgTX binding were identified. The highest binding density was found in the 6D94 subline which has a B_{max} of 80 000 sites/cell as determined by saturation studies with [^{125}I]MgTX. Western blot analysis using a sequence-specific anti-$K_V1.3$ antibody reveals that the transfected line has high levels of immunoreactivity for $K_V1.3$ while it was undetectable in nontransfected CHO cells (Figure 5). No immunoreactivity was found by Western blots employing site-directed antibodies raised against $K_V1.1$, $K_V1.2$, $K_V1.4$, or $K_V1.6$ channels (data not shown). These data indicate that, as expected, $K_V1.3$ is the only voltage-gated potassium channel of the *Shaker* family expressed in the CHO cell line.

[^{125}I]MgTX binding to CHO/K_V1.3 membranes is similar to that for binding to Jurkat membranes, except for the observation of the predicted higher site density (B_{max} of 750 fmol/mg) and the expected higher signal to noise ratio (Figure 2, lower panels). There is no displaceable [^{125}I]MgTX binding to membranes prepared from nontransfected cells (data not shown). The K_d, at 190 fM (average of 140 ± 42 fM), is slightly higher than that for Jurkat membranes (95 fM). The K_d's measured in both CHO/K_V1.3 and Jurkat are similar to the values obtained from rat brain membranes in which the equilibrium binding value was 180 fM (Knaus et al., 1995).

The kinetics for [^{125}I]MgTX binding to CHO/K_V1.3 membranes are shown in Figure 5. The association was determined for 140 fM ligand. The pseudo-first-order linear

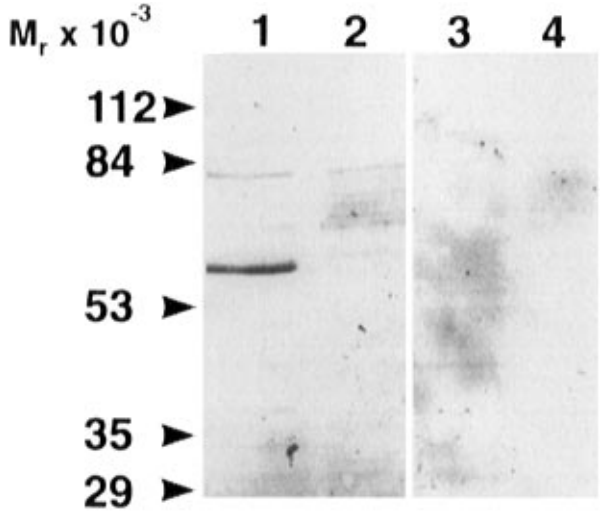

FIGURE 6: Western blot analysis for the presence of $K_V1.3$ in plasma membranes prepared from CHO/$K_V1.3$ cells. CHO/$K_V1.3$ (lanes 1 and 2) or nontransfected CHO (lanes 3 and 4) membranes (~20 μg/lane) were separated on a 12% SDS/PAGE, transferred to a PVDF membrane, and visualized by immunoblotting with anti-$K_V1.3$(456−474) as described in Materials and Methods. Lanes 1 and 3 show control immunostaining, and lanes 2 and 4 show staining in the presence of the 1 μM corresponding antigenic peptide. The apparent M_r's of the employed protein standards are indicated by arrowheads. The apparent M_r of the $K_V1.3$ protein was estimated to be 59 kDa.

transformation results in a k_{obs} of 0.189 min^{-1}. The k_{-1} from the dissociation experiment was 0.108 min^{-1}. When corrected for the dissociation and the concentration used, the k_1 from the association experiment was 0.000 579 min^{-1} fM^{-1}, which resulted in a K_d of 187 fM. This value was well within the range of K_d's obtained through equilibrium binding experiments.

The salt dependence of [^{125}I]MgTX binding to CHO/$K_V1.3$ membranes is similar to that for binding to Jurkat membranes. In this respect, there is an absolute requirement for K^+ to facilitate toxin binding (half-maximal stimulation is 0.53 mM) and no stimulation by NaCl is observed at any concentration tested (Figure 4, lower panel). At a high salt concentration with 100 mM NaCl and 4.6 mM KCl, the K_d rises to 50 pM for CHO/$K_V1.3$ (Figure 3, lower panels). The B_{max} for this CHO/$K_V1.3$ membrane preparation at 1200 fmol/mg was somewhat higher than the one shown for the preparation used in Figure 2 (lower panels). In CHO/$K_V1.3$ membranes, as with that in Jurkat and similar to that in brain, addition of either KCl or NaCl in the presence of a maximally stimulating concentration of KCl inhibits [^{125}I]MgTX binding above 5 mM for either salt with IC_{50}'s of 19 and 13 mM, respectively (Figure 4).

Immunocytochemical Analysis of the Jurkat [^{125}I]MgTX Receptor. The Western blot analysis of plasma membranes prepared from CHO cells (Figure 6) shows that only the $K_V1.3$ transfected cells respond to the anti-$K_V1.3$ antibody. The M_r of 59 kDa corresponds to that expected for a single subunit of $K_V1.3$ (Stuhmer et al., 1989; Swanson et al., 1990).

Since the site density of Jurkat membranes is too low to facilitate a Western blot analysis with any confidence, antibodies to K_V1 series channels were employed for immunoprecipitation studies of the [^{125}I]MgTX receptor. Solubilized [^{125}I]MgTX receptors from Jurkat membranes can be precipitated only by anti-$K_V1.3$ antibodies but not by anti-$K_V1.1$, -1.2, -1.4, or -1.6 antibodies (data not shown). These experiments indicate that the [^{125}I]MgTX receptor of Jurkat membranes is most likely a homomultimer of $K_V1.3$. This observation is in contrast to a similar analysis performed with rat brain synaptic membranes, where either anti-$K_V1.2$ or anti-$K_V1.3$ precipitate solubilized [^{125}I]MgTX receptors, indicating that the receptor in brain is a heteromultimer of at least $K_V1.2$ and $K_V1.3$ subunits (Knaus et al., 1995).

Table 1: Effects of Toxins on Binding of [^{125}I]MgTX and $^{86}Rb^+$ Efflux[a]

	IC_{50} pM				
	Jurkat	CHO/$K_V1.3$		Brain[b]	$^{86}Rb^+$
peptide	low salt	low salt	high salt	low salt	efflux
ChTX	1.2	2.1	99	11	2100
MgTX	0.10	0.17	11	0.37	110
AgTX-1	0.23	0.42	110	0.22	1100
AgTX-2	0.27	NT	84	0.64	NT
NxTX	0.53	NT	48	NT	1200
KTX	3.1	2.3	470	NT	3800
α-DaTX	14 000	4100	270 000	0.84	no effect
IbTX	no effect on any assay up to 100 nM				

[a] NT, not tested. Peptidyl inhibitors of K_V1 series channels were tested for block in several assays: [^{125}I]MgTX binding to plasma membranes prepared from Jurkat or CHO/$K_V1.3$ cells and $^{86}Rb^+$ efflux from CHO/$K_V1.3$ cells activated by depolarizing with K^+_o. These data are compared with previously reported (Knaus et al., 1995) data for [^{125}I]MgTX binding to rat brain synaptic membranes. [b] Knaus et al. (1995).

Pharmacology of the [^{125}I]MgTX Receptor. Several peptide toxins have previously been characterized that define a spectrum of potencies in inhibiting different K_V1 series channels (Garcia et al., 1991, 1994; Grissmer et al., 1994; Laraba-Djebari et al., 1994). These toxins were compared for inhibition of [^{125}I]MgTX binding in low-salt Tris binding buffer in the presence of 3 mM KCl. While these toxins showed a range of potencies, the IC_{50}'s for each of these toxins were similar for either Jurkat or CHO/$K_V1.3$ membranes (Table 1). MgTX is the most potent competitor, followed closely by agitoxin-1, agitoxin-2, and noxiustoxin. ChTX and kaliotoxin are somewhat less potent, while α-dendrotoxin is very weak. Iberiotoxin, which has 78% sequence identity with ChTX but does not block K_V1 series channels, has no observable effect on any of these assays. There are some differences among the scorpion toxins when they are tested against [^{125}I]MgTX binding to rat brain membranes in low-salt buffer without KCl present, but they are not particularly large when standardized against Jurkat or CHO/$K_V1.3$ [^{125}I]MgTX binding results. In contrast, the snake venom peptide, α-DaTX, is far more potent at blocking [^{125}I]MgTX binding to brain than it is at blocking binding to either Jurkat or CHO/$K_V1.3$ membranes. In high-salt binding buffer with 100 mM NaCl present, the relative potencies of these peptides as compared to that of MgTX for inhibition of [^{125}I]MgTX binding to CHO/$K_V1.3$ are maintained within a factor 3 or 4 as compared to the potency ratios determined in low salt for either Jurkat or CHO/$K_V1.3$ membranes. It might be expected that the binding affinities of the toxins with their diverse charge densities would be affected in somewhat different ways by ionic strength, thus accounting for the modest change in potency ratios observed in high salt.

When the inhibition of $^{86}Rb^+$ efflux from CHO/$K_V1.3$ cells by different peptides is compared with their ability to inhibit [^{125}I]MgTX binding to CHO/$K_V1.3$ membranes in high salt, there is an about 10-fold loss in potency for most of the peptides, but the basic relative potencies of inhibition are

preserved (Table 1). There appears, then, to be a strong correlation between the ability of these peptides to inhibit [^{125}I]MgTX binding to Jurkat or CHO/$K_V1.3$ membranes and their ability to inhibit $^{86}Rb^+$ efflux through $K_V1.3$ channels. The major discriminator among these assays is α-DaTX, which shows very potent effects only on MgTX binding in brain, while exhibiting weak effects on [^{125}I]MgTX binding to Jurkat and CHO/$K_V1.3$ membranes, as well as having no effect on $^{86}Rb^+$ efflux from CHO/$K_V1.3$ cells. These results would be consistent with the different proposed channel subunit compositions in rat brain as compared to the other two membrane preparations.

DISCUSSION

The data presented in this paper indicate that the voltage-gated K^+ channels present in Jurkat cells, a surrogate for human peripheral blood T cells, are comprised of homomultimers of $K_V1.3$. Evidence which supports this conclusion is the similarity between the properties of the [^{125}I]-MgTX binding sites in plasma membranes prepared either from Jurkat cells or from a CHO cell line which stably expresses homomultimeric $K_V1.3$ channels. The affinities, the absolute requirement for the presence of low millimolar concentrations of KCl, the lack of stimulation by any concentration of NaCl tested, and the inhibition at high concentrations of KCl and NaCl are properties of [^{125}I]MgTX binding which are identical for Jurkat and CHO/$K_V1.3$ membranes. The potency pattern for inhibition of [^{125}I]-MgTX binding by a series of peptide toxins indicates that the molecular pharmacology of these two receptors is the same. In these respects, the characteristics of [^{125}I]MgTX binding are identical for binding of the peptide to Jurkat plasma membranes and to CHO cells that have only $K_V1.3$ present. Germane to this comparison, it should be noted that, of the anti-K_V1 series antibodies tested, only anti-$K_V1.3$ was able to immunoprecipitate solubilized [^{125}I]MgTX receptors from Jurkat.

The observation that there is an absolute requirement for K^+ to facilitate binding of [^{125}I]MgTX to Jurkat or CHO/$K_V1.3$ is intriguing. It has previously been shown that certain channels such as $K_V1.3$ and $K_V1.4$ do not conduct K^+ from the inside in the absence of extracellular K^+ (Pardo et al., 1992). This effect is completely reversed by the addition of extracellular K^+. However, $K_V1.4$ still exhibits gating currents under limiting K^+_o conditions. For $K_V1.4$, the K^+_o concentration at which half of the maximal amplitude was obtained is around 2.2 mM, similar to the level of K^+ required for $K_V1.3$. The effects of extracellular K^+ on $K_V1.4$ have been localized to a residue that confers TEA sensitivity to K^+ channels. The corresponding residue in $K_V1.3$, H404, has been shown to be involved in the interaction of kaliotoxin and in the C-type inactivation of the channel (Aiyar et al., 1995; Busch et al., 1991). It is tempting to speculate that modulation of [^{125}I]MgTX binding to $K_V1.3$ by K^+ is related to the effects of external K^+ on ion permeation, where, in the absence of K^+, the channel may be locked into a low-affinity conformation for [^{125}I]MgTX.

Inhibition of [^{125}I]MgTX binding by K^+ and Na^+ at concentrations above 10 mM may reflect a simple ionic strength effect. The IC_{50}'s for these two monovalent cations are within a factor of 2 for each other, with Na^+ being the more potent on both Jurkat and CHO/$K_V1.3$ membranes. This weaker K^+ effect, if significant, may reflect a crossover between the effects of additional stimulation as K^+ is increased, negating some of the inhibitory effects at higher concentrations. There is also an apparent 2-fold weaker effect of K^+ and Na^+ in inhibiting [^{125}I]MgTX binding to Jurkat membranes as compared to that of CHO/$K_V1.3$ membranes. Such differences may not be significant within experimental error or, if real, may reflect some subtle differences between the expressed and native channels.

The high-affinity [^{125}I]MgTX binding site previously characterized in rat brain has been shown to be a heteromultimer consisting of at least $K_V1.2$ and $K_V1.3$ subunits (Knaus et al., 1995). Antibodies directed against either $K_V1.2$ or $K_V1.3$ precipitate [^{125}I]MgTX receptors from solubilized synaptic membranes. In Jurkat membranes, however, only $K_V1.3$ antibodies are able to immunoprecipitate solubilized [^{125}I]MgTX receptors. Other significant differences from Jurkat and CHO/$K_V1.3$ membranes are that, although [^{125}I]MgTX binding to brain is stimulated by KCl, there is no absolute requirement for KCl and there is modest enhancement by low concentrations of NaCl. The most significant difference between brain and Jurkat or CHO/$K_V1.3$ receptors resides in the pharmacological sensitivity of [^{125}I]MgTX binding in rat brain membranes to α-DaTX. The α-DaTX binding data is particularly important in view of the high potency of this toxin against $K_V1.1$, -1.2, and -1.6 channels and its weak effect against $K_V1.3$ (Grissmer et al., 1994; Pongs, 1992). It also should be noted that the presence of $K_V1.3$ in the heteromultimer comprising the [^{125}I]-MgTX receptor in brain does not block the binding of α-DaTX. The immunoprecipitation experiments together with the low potency of inhibition by α-DaTX of [^{125}I]MgTX binding to Jurkat membranes would suggest that $K_V1.1$, -1.2, -1.4, and -1.6 are not part of the receptor in these cells.

It could still be argued that [^{125}I]MgTX binding sites in Jurkat might be comprised of additional K_V subunits that are novel with no known selective ligand or whose antibodies were not available for testing in these experiments. For $K_V1.5$, in particular, no antibody was available for use in immunoprecipitation experiments, no potent peptidyl inhibitor has been reported, and the peptides tested in our experiments are all relatively weak at blocking this channel. However, it has been shown that, when $K_V1.5$ is coexpressed with toxin-sensitive subunits, the channel complex loses its toxin sensitivity, presumably because bulky residues in the H5 region of $K_V1.5$ sterically prevent toxin binding in the pore of the channel complex (Overturf et al., 1994). Without the development of more potent ligands or antibodies for $K_V1.5$, it would be difficult to rule out the presence of this subunit in Jurkat by binding experiments alone. However, its presence is highly unlikely because there is no evidence for the presence of $K_V1.5$ in Jurkat cells with either electrophysiological (Attali et al., 1992) or Northern blot analysis (Chandy & Gutman, 1995).

Overall, the weight of the evidence indicates that [^{125}I]-MgTX binding to Jurkat plasma membranes is most probably to homomultimeric $K_V1.3$ channels since the characteristics of binding are the same for the homomultimeric channels of CHO/$K_V1.3$ membranes. These data are consistent with previous reports identifying the human T cell voltage-gated K^+ channel as $K_V1.3$ (Cai et al., 1992; Douglass et al., 1990). The difference between the configuration of K_V channels in brain and in lymphocytes suggests that homomultimeric $K_V1.3$ in human T cells may be relatively unique. The caveat is that $K_V1.3$ has also been reported in other hematopoetically

derived cells (Gallin, 1984; Mahaut-Smith et al., 1990, Partiseti et al., 1992), osteoclasts (Arkett et al., 1994), and fibroblasts (Grissmer et al., 1990), although the makeup of the channel has not yet been fully described for these tissues.

Inhibitors of $K_V1.3$ may be potentially useful in the development of immunosuppressants because of their demonstrated block of activation of human T cells (Lin et al., 1993) and, more recently, their suppression of a delayed-type hypersensitivity reaction in Yucatan minipigs (Koo et al., 1996). Nonetheless, reports persist where $K_V1.3$ inhibitors like kaliotoxin fail to block human T cell activation (Rader et al., 1996). It should be noted that there is a marked dependence of the effectiveness of $K_V1.3$ inhibitors on the level of stimulation encountered: the activation of T cells at maximal stimuli cannot be overcome by the peptides, whereas at lower stimulus levels, T cell proliferation can be blocked to a very high degree (Lin et al., 1993). This observation may be due to the elevation of Ca^{2+}_i via other pathways in the presence of strong stimuli which would not be blocked by an intervention that affects cellular polarization levels.

MgTX, which blocks human peripheral blood T lymphocyte activation through inhibition of $K_V1.3$, has been a useful tool for the study of the role of this channel in T cell activation. Establishing that $K_V1.3$ exists as a homomultimer in T cells, in contrast with brain, may provide a basis for intervention at this channel to produce an immunosuppressant with significant tissue selectivity. [^{125}I]MgTX is a powerful, new probe that will allow further study of $K_V1.3$ channels and better definition of their role in T cell activation.

ACKNOWLEDGMENT

We thank Ms. Tracey D. Klatt for her help with mass spectral analysis of MgTX and its iodinated derivatives.

REFERENCES

Aiyar, J., Withka, J. M., Rizzi, J. P., Singleton, D. H., Andrews, G. C., Lin, W., Boyd, J., Hanson, D. C., Simon, M., Dethlefs, B., Lee, C.-L., Hall, J. E., Gutman, G. A., & Chandy, K. G. (1995) *Neuron 15*, 1169−1181.

Arkett, S. A., Dixon, J., Yang, J. N., Sakai, D. D., Minkin, C., & Sims, S. M. (1994) *Recept. Channels 2*, 281−293.

Attali, B., Romey, G., Honore, E., Schmidalliana, A., Mattei, M. G., Lesage, F., Ricard, P., Barhanin, J., & Lazdunski, M. (1992) *J. Biol. Chem. 267*, 8650−8657.

Bednarek, M. A., Bugianesi, R. M., Leonard, R. J., & Felix, J. P. (1994) *Biochem. Biophys. Res. Commun. 198*, 619−625.

Busch, A. E., Hurst, R. S., North, R. A., Adelman, J. P., & Kavanaugh, M. P. (1991) *Biochem. Biophys. Res. Commun. 179*, 1384−1390.

Cai, Y. C., Osborne, P. B., North, R. A., Dooley, D. C., & Douglass, J. (1992) *DNA Cell Biol. 11*, 163−172.

Chandy, K. G., & Gutman, G. A. (1995) in *Handbook of Receptors and Channels* (North, R. A., Ed.) CRC Press, Boca Raton, FL.

Chandy, K. G., Williams, C. B., Spencer, R. H., Aguilar, B. A., Ghanshani, S., Tempel, B. I., & Gutman, G. A. (1990) *Science 247*, 973−975.

Cheng, Y.-C., & Prusoff, W. H. (1973) *Biochem. Pharmacol. 22*, 3099−3108.

DeFarias, F. P., Stevens, S. P., & Leonard, R. J. (1995) *Recept. Channels 3*, 273−281.

Deutsch, C., Price, M., Lee, S., King, V. F., & Garcia, M. L. (1991) *J. Biol. Chem. 266*, 3668−3674.

Douglass, J., Osborne, P. B., Cai, Y.-C., Wilkinson, M., Christie, M. J., & Adelman, J. P. (1990) *J. Immunol. 144*, 4841−4850.

Felix, J. P., Bugianesi, R. M., Abramsom, A. A., & Slaughter, R. S. (1995) *Biophys. J. 68*, 267a.

Gallin, E. K. (1984) *Biophys. J. 46*, 821−825.

Garcia, M. L., Galvez, A., Garcia-Calvo, M., King, V. F., Vazquez, J., & Kaczorowski, G. J. (1991) *J. Bioenerg. Biomembr. 23*, 615−646.

Garcia, M. L., Garcia-Calvo, M., Hidalgo, P., Lee, A., & MacKinnon, R. (1994) *Biochemistry 33*, 6834−6839.

Garcia-Calvo, M., Leonard, R. J., Novick, J., Stevens, S. P., Schmalhofer, W., Kaczorowski, G. J., & Garcia, M. L. (1993) *J. Biol. Chem. 268*, 18866−18874.

Grissmer, S., Dethlefs, B., Wasmuth, J. J., Goldin, A. L., Gutman, G. A., Cahalan, M. D., & Chandy, K. G. (1990) *Proc. Natl. Acad. Sci. U.S.A. 87*, 9411−9415.

Grissmer, S., Nguyen, A. N., Aiyar, J., Hanson, D. C., Mather, R. J., Gutman, G. A., Karmilowicz, M. J., Auperin, D. D., & Chandy, K. G. (1994) *Mol. Pharmacol. 45*, 1227−1234.

Knaus, H.-G., Koch, R. O. A., Eberhart, A., Kaczorowski, G. J., Garcia, M. L., & Slaughter, R. S. (1995) *Biochemistry 34*, 13627−13634.

Koo, G. C., Blake, J. T., Talento, A., Nguyen, M., Lin, S., Sirotina, A., Shah, K., Mulvany, K., Hora, D., Jr., Cunningham, P., Slaughter, R., Bugianesi, R., Felix, J., Garcia, M., Williamson, J., Kaczorowski, G., Sigal, N., Springer, M., & Feeney, W. (1996) *FASEB J. 10*, A1447.

Laraba-Djebari, F., Legros, C., Crest, M., Ceard, B., Romi, R., Mansuelle, P., Jacquet, G., Rietschoten, J. v., Gola, M., Rochat, H., Bougis, P. E., & Martin-Eauclaire, M.-F. (1994) *J. Biol. Chem. 269*, 32835−32843.

Leonard, R. J., Garcia, M. L., Slaughter, R. S., & Reuben, J. P. (1992) *Proc. Natl. Acad. Sci. U.S.A. 89*, 10094−10098.

Lewis, R. S., & Cahalan, M. D. (1990) *Annu. Rev. Physiol. 52*, 415−430.

Lin, C. S., Boltz, R. C., Blake, J. T., Nguyen, M., Talento, A., Fischer, P. A., Springer, M. S., Sigal, N. H., Slaughter, R. S., Garcia, M. L., Kaczorowski, G. J., & Koo, G. C. (1993) *J. Exp. Med. 177*, 637−645.

Mahaut-Smith, M. P., Rink, T. J., Collins, S. C., & Sage, S. O. (1990) *J. Physiol. (London) 428*, 723−735.

Newman, M. J., Foster, D. L., Wilson, T. H., & Kaback, H. R. (1982) *J. Biol. Chem. 256*, 11804−11808.

Overturf, K. E., Russell, S. N., Carl, A., Vogalis, F., Hart, P. J., Hume, J. R., Sanders, K. M., & Horowitz, B. (1994) *Am. J. Physiol. 36*, C1231−C1238.

Pardo, L. A., Heinemann, S. H., Terlau, H., Ludewig, U., Lorra, C., Pongs, O., & Stuhmer, W. (1992) *Proc. Natl. Acad. Sci. U.S.A. 89*, 2466−2470.

Partiseti, M., Choquet, D., Diu, A., & Korn, H. (1992) *J. Immunol. 148*, 3361−3368.

Pongs, O. (1992) *Trends Pharmacol. Sci. 13*, 359−365.

Price, M., Lee, S. C., & Deutsch, C. (1989) *Proc. Natl. Acad. Sci. U.S.A. 86*, 10171−10175.

Rader, R. K., Kahn, L. E., Anderson, G. D., Martin, C. L., Chinn, K. S., & Gregory, S. A. (1996) *J. Immunol. 156*, 1425−1430.

Schaffner, W., & Weissmann, C. (1973) *Anal. Biochem. 56*, 502−514.

Slaughter, R. S., Shevell, J. L., Felix, J. P., Lin, C. S., Sigal, N. H., & Kaczorowski, G. J. (1991) *Biophys. J. 59*, 213a.

Stuhmer, W., Ruppersberg, J. P., Schroter, K. H., Sakmann, B., Stocker, M., Giese, K. P., Perschke, A., Baumann, A., & Pongs, O. (1989) *EMBO J. 8*, 3235−3244.

Sun, T., Naini, A. A., & Miller, C. (1994) *Biochemistry 33*, 9992−9999.

Swanson, R., Marshall, J., Smith, J. S., Williams, J. B., Boyle, M. B., Folander, K., Luneau, C. J., Antanavage, J., Oliva, C., Buhrow, S. A., Bennett, C., Stein, R. B., & Kaczmarek, L. K. (1990) *Neuron 4*, 929−939.

BI962351P